

Sensitivity and Consistency Studies of Muon Arrival Time Distributions Measured by KASCADE

A.F. Badea^{a*†}, T. Antoni^a, W.D. Apel^b, K. Bekk^b, A. Bercuci^{b†}, H. Blümer^{b,a}, H. Bozdog^b, I.M. Brancus^c, C. Büttner^a, A. Chilingarian^d, K. Daumiller^a, P. Doll^b, J. Engler^b, F. Feßler^b, H.J. Gils^b, R. Glasstetter^a, R. Haeusler^a, A. Haungs^b, D. Heck^b, J.R. Hörandel^a, A. Iwan^{a‡}, K.-H. Kampert^{a,b}, H.O. Klages^b, G. Maier^b, H.J. Mathes^b, H.J. Mayer^b, J. Milke^b, M. Müller^b, R. Obenland^b, J. Oehlschläger^b, S. Ostapchenko^{a§}, M. Petcu^c, H. Rebel^b, M. Risse^b, M. Roth^b, G. Schatz^b, H. Schieler^b, J. Scholz^b, T. Thouw^b, H. Ulrich^a, J.H. Weber^a, A. Weindl^b, J. Wentz^b, J. Wochele^b, J. Zabierowski^e

^aInstitut für Experimentelle Kernphysik, Universität Karlsruhe, 76021 Karlsruhe, Germany

^bInstitut für Kernphysik, Forschungszentrum Karlsruhe, 76021 Karlsruhe, Germany

^cNational Institute of Physics and Nuclear Engineering, 7690 Bucharest, Romania

^dCosmic Ray Division, Yerevan Physics Institute, Yerevan 36, Armenia

^eSoltan Institute for Nuclear Studies, 90950 Lodz, Poland

Using the facilities of the KASCADE Central Detector EAS muon arrival time distributions, observed with reference to the arrival time of the first locally registered muon, and their correlations with other EAS observables have been investigated at different distances R_μ from the shower axis. Invoking detailed Monte Carlo simulations non-parametric multivariate even-by-event analyses have been performed for an estimate of the primary mass composition. The consistency of the Monte Carlo simulations is studied by comparing the primary mass composition results inferred from observations at different R_μ and different muon multiplicity thresholds n_{th} .

1. Muon arrival time distributions

KASCADE [1] is a multidetector system, installed in Forschungszentrum Karlsruhe (110 m a.s.l.), Germany, for the observation of extensive air showers in the primary energy range around the *knee*. The field array of 252

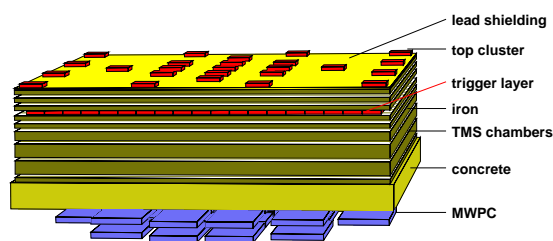


Figure 1. KASCADE Central Detector.

*corresponding author, e-mail: Florin.Badea@ik.fzk.de

†on leave of absence from National Institute of Physics and Nuclear Engineering, Bucharest, Romania

‡on leave of absence from University of Lodz, Poland

§on leave of absence from Moscow State University Moscow, Russia

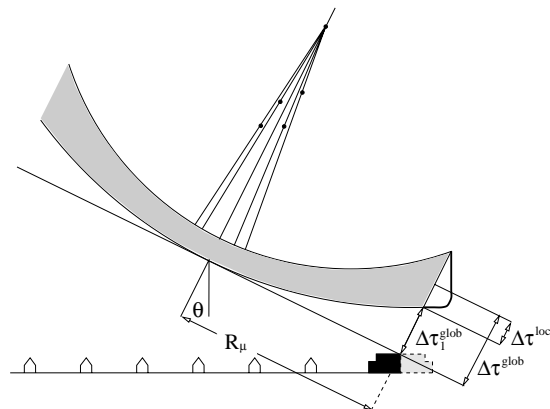


Figure 2. Characterisation of the EAS temporal structure by global and local arrival times.

detector stations, distributed over an area of $200 \times 200 \text{ m}^2$, measures the electron-photon component ($E_{th} = 5 \text{ MeV}$) and the muon component with an energy threshold of 230 MeV . It provides the basic information about arrival direction, core position, electron and muon sizes of the observed EAS. In particular, from the data of the field array the so-called truncated muon

number N_μ^{tr} , i.e. the muon density integrated between 40 m and 200 m is derived and used at KASCADE as an approximate mass independent primary energy identifier. The muon arrival time measurements use the facilities of the Central Detector (see Fig. 1) of KASCADE [2]. It is basically an iron sampling calorimeter ($16 \times 20 \text{ m}^2$) for the measurement of EAS hadrons. In the basement of the set-up, below 3800 t of iron and concrete, large-area position-sensitive multiwire proportional chambers (MWPC) [3] are operated for the identification of muons with 2.4 GeV energy threshold. The trigger plane of the calorimeter is a system of 456 plastic scintillation detector elements for providing a fast trigger signal for the MWPC, and for the timing measurements. The muon arrival time distributions measured by the trigger layer combined with the muon identification by the MWPC facilities are the focus of this work. Measured arrival times $\tau_{1\mu} < \tau_{2\mu} < \tau_{3\mu} < \dots$ of muons registered by timing detectors at a distance R_μ from the shower axis, corrected by $\pm R_\mu \tan \theta / c$ (c - speed of light) in order to eliminate the distortions due to the shower inclination (see Fig. 2), refer to an experimentally provided zero-time. The present analysis uses "local" times, which refer to the arrival of the foremost muon locally registered by the detector, informing about the thickness and the structure of the muon disc. For event-by-event observations with a fluctuating number of muons (multiplicity n), the individual relative arrival time distributions can be characterised by the mean values $\Delta\tau_{mean}$, and by various quantiles $\Delta\tau_q$, like the median $\Delta\tau_{0.50}$, the first quartile $\Delta\tau_{0.25}$ and the third quartile $\Delta\tau_{0.75}$ [4].

2. Comparison between experimental and simulated data

An amount of 24 millions experimentally observed air-shower events have been analysed [5]. Muon arrival time distributions have been reconstructed for shower events with a multiplicity number of $n \geq 3$ of registered muons with the energy threshold $E_{th} = 2.4 \text{ GeV}$; after applying some general cuts concerning the core position (within 100 m from the array centre), the

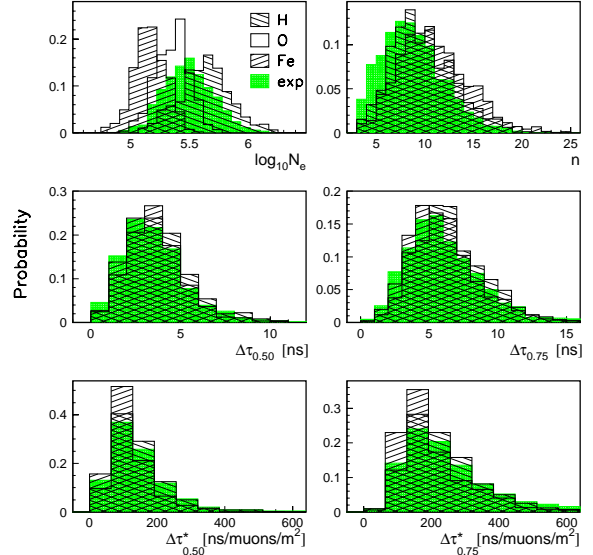


Figure 3. Simulated and experimental EAS observable distributions for $4.05 < \log_{10} N_\mu^{tr} \leq 4.28$, $80 \text{ m} < R_\mu \leq 90 \text{ m}$ and $0^\circ \leq \theta \leq 24^\circ$.

angle of EAS incidence θ ($< 40^\circ$) and $\log_{10} N_\mu^{tr}$ (> 3.6) the sample shrank to approx. 240 000 showers. The present analysis is based on simulations with the code CORSIKA (version 5.62) [6] with a full and detailed simulation of the detector response. The simulations use the QGSJET (version 1998) model [7] as generator for high-energy hadronic interactions and GHEISHA [8] for interactions below $E_{lab} = 80 \text{ GeV}$. The electromagnetic part is treated by the EGS4 program [9]. The simulations have been performed for three different classes of primaries: protons (H), oxygen (O), and iron (Fe). The energy range covered by the simulations extends from $5.0 \cdot 10^{14} \text{ eV}$ to $3.06 \cdot 10^{16} \text{ eV}$ with a fixed spectral index $\gamma = -2.7$ adopted for all primaries and the zenith angles comprise the range of $0^\circ \leq \theta \leq 40^\circ$ [5]. For each primary type approximately 90 000 showers have been simulated. Fig. 3 displays frequency distributions of some shower parameters as predicted by the simulation for different primaries and compared to the actual experimental observations for a particular $\log_{10} N_\mu^{tr}$ and R_μ bin. The $\Delta\tau_q^* = \Delta\tau_q / \rho_\mu$ are the reduced quantiles of the local muon arrival time distributions ($E_{th} = 2.4 \text{ GeV}$). Density of muons ρ_μ is

the observed muon multiplicity n divided by the effective area of the muon detector set-up. $\Delta\tau_q^*$ provide even more pure arrival time information than $\Delta\tau_q$ because $1/\rho_\mu$ works like a correction factor decreasing the fluctuations of the local time parameters originating from the multiplicity dependence [10].

3. Sensitivity of muon arrival times distributions to the primary mass

Non-parametric statistical methods are applied in studies of multidimensional distributions of observables allocating the single observed events to different classes by comparing the observed events with the simulated distributions without using a pre-chosen parameterisation [11]. The procedures take into account the effects of the EAS fluctuations in a quite natural way and are able to specify the uncertainties, by an estimate of the true-classification and misclassification probabilities. Fig. 4 shows as variation with $\log_{10}N_\mu^{tr}$ the true-classification probabilities (and uncertainties) averaged over all classes. With little surprise it is noted that the mass discrimination is dominated by the $\{N_\mu^{tr}, N_e\}$ correlation and improving with primary energy. It is also evident that by adding the correlation of the reduced values of the local time parameters (median $\Delta\tau_{0.50}$ or the third quartile $\Delta\tau_{0.75}$) a marginal but systematic improvement is obtained.

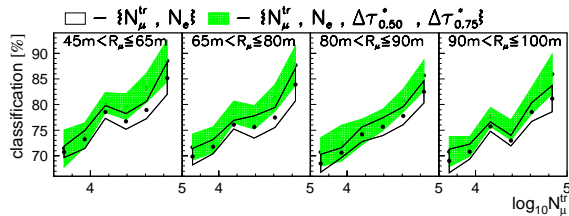


Figure 4. The dependence of the averaged true-classification probability from $\{N_\mu^{tr}, N_e\}$ and $\{N_\mu^{tr}, N_e, \Delta\tau_{0.50}^*, \Delta\tau_{0.75}^*\}$ correlations; $0^\circ \leq \theta \leq 24^\circ$.

4. Test of the consistency of Monte Carlo simulations

The analysis of the EAS observations introduces necessarily some model dependence by the high-

energy hadronic interaction models invoked as generators of the Monte Carlo simulations. A possible way to evaluate the quality of a model is to derive the primary mass composition from the analysis of a certain set of observables (the set $\{N_\mu^{tr}, N_e, \Delta\tau_{0.50}^*, \Delta\tau_{0.75}^*\}$ has been furtheron used) in different $\{\log_{10}N_\mu^{tr}, R_\mu\}$ ranges; the consistency test in this case is the invariance of the primary mass composition over the R_μ ranges. The true-classification $P_{i \rightarrow i}$ and misclassification $P_{i \rightarrow j}$ probabilities ($i, j \in \{H, O, Fe\}$), deduced for all studied $\{\log_{10}N_\mu^{tr}, R_\mu\}$ ranges, are used for the reconstruction of the mass composition of the samples of registered events by inverting a system of linear equations [12]. The result of the application of the reconstruction procedures to experimental samples observed at different distances R_μ from the shower centre, are shown in the upper panels of Fig. 5. The mass compositions (P_H, P_O, P_{Fe}) of measured KASCADE samples differ for different R_μ bins, since the observation conditions lead to mass dependent differences in the observation efficiency at different R_μ . Efficiency correction factors (C_H, C_O, C_{Fe}) have been calculated from the Monte-Carlo simulations in order to adjust the mass composition of measured samples (P_H, P_O, P_{Fe}) to the primary mass composition (P_H^*, P_O^*, P_{Fe}^*) according to the relation [5]:

$$P_H^* : P_O^* : P_{Fe}^* = \frac{P_H}{C_H} : \frac{P_O}{C_O} : \frac{P_{Fe}}{C_{Fe}}. \quad (1)$$

The $\log_{10}N_\mu^{tr}$ -variation of the primary mass composition resulting after the correction concerning the biased acceptance by the specific observational conditions is shown in the lower part of Fig. 5. In Fig. 6 the results are shown as variation with R_μ for different $\log_{10}N_\mu^{tr}$ ranges. A more stringent test of the Monte Carlo simulations (use both for classification procedure and calculation of the efficiency correction factors) is to scrutinise not only the variation with R_μ but also the dependence with the multiplicity threshold n_{th} of the reconstructed primary mass composition. Fig. 7 shows this aspect for a certain $\log_{10}N_\mu^{tr}$ range.

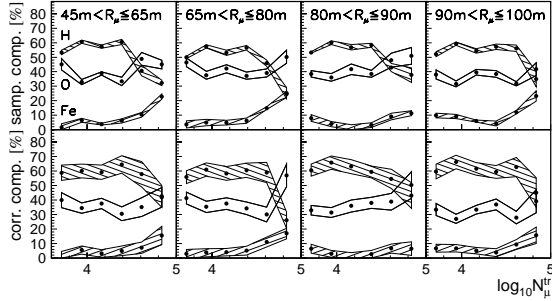


Figure 5. Variation of the measured and efficiency corrected mass compositions with $\log_{10} N_{\mu}^{tr}$ for various R_{μ} ranges; $0^{\circ} \leq \theta \leq 24^{\circ}$.

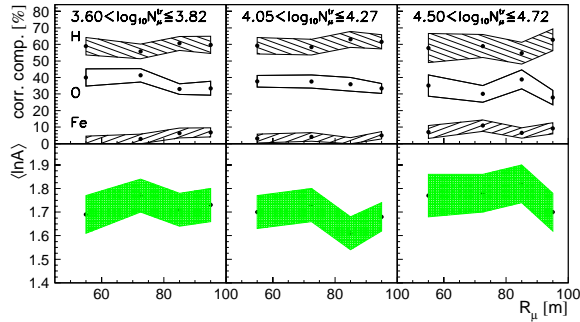


Figure 6. Variation of the efficiency corrected mass composition and of $\langle \ln A \rangle$ with R_{μ} for various $\log_{10} N_{\mu}^{tr}$ ranges; $0^{\circ} \leq \theta \leq 24^{\circ}$.

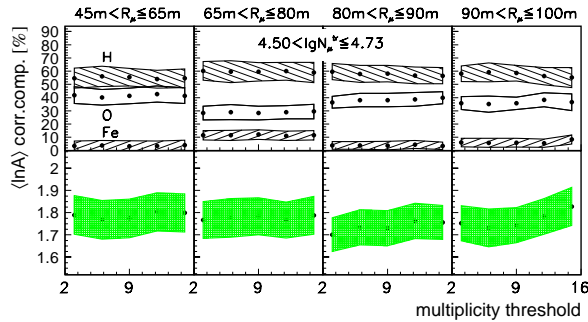


Figure 7. Variation of the efficiency corrected mass composition with the multiplicity threshold n_{th} using the $\{N_{\mu}^{tr}, N_e\}$ correlation for the non-parametric classification procedure of the events observed at different distances from the shower axis; $0^{\circ} \leq \theta \leq 24^{\circ}$.

5. Conclusions

The local time quantities provide only a marginal contribution to the mass discrimination as

compared to the dominant $\{N_{\mu}^{tr}, N_e\}$ correlation, at least in the relatively limited range of $R_{\mu} < 100$ m and $E_0 < 10^{16}$ eV. The present observations corroborate the findings of an increase of $\langle \ln A \rangle$ beyond the knee, i.e. for $\log_{10} N_{\mu}^{tr} > \text{ca. } 4.2$. By applying the calculated correction factors to the results found at *different* R_{μ} and n_{th} the resulting mass composition is almost invariant; the result indicates a good consistency of the performed Monte Carlo simulations using the QGSJET model as generator.

Acknowledgement *The KASCADE experiment is supported by WTZ projects in the frame of the scientific-technical cooperation between Germany and Romania (RUM 97/014), Poland (POL 99/005) and Armenia (ARM 98/002). The Polish group (Soltan Institute and University of Lodz) acknowledges the support by the Polish State Committee for Scientific Research (grant No. 5 P03B 133 20).*

REFERENCES

1. H.O. Klages et al. - KASCADE Coll., *Nucl. Phys. B (Proc. Suppl.)* **52B** (1997) 92
2. J. Engler et al., *Nucl. Instr. and Meth.* **A 427** (1999) 528
3. H. Bozdog et al., *Nucl. Instr. and Meth.* **A 465** (2001) 45
4. T. Antoni et al. - KASCADE Collaboration, *Astrop. Phys.* **15** (2001) 149
5. A.F. Badea, *FZKA-Report 6579*, Forschungszentrum Karlsruhe (2001)
6. D. Heck et al., *FZKA-Report 6019*, Forschungszentrum Karlsruhe (1998)
7. N.N. Kalmykov et al., *Nucl. Phys. B (Proc. Suppl.)* **52B** (1997) 17
8. H. Fesefeldt, *PITHA - 85/02*, RWTH Aachen (1985)
9. W.R. Nelson et al., *Report SLAC 265*, Stanford Linear Accelerator Center (1985)
10. R. Haeusler et al., *Astrop. Phys.* **17** (2002) 421
11. A.A. Chilingarian, *Comp. Phys. Comm.* **54** (1989) 381; A.A. Chilingarian and G.Z. Zazian, *Nuovo Cim.* **14** (1991) 355; *ANI reference manual*, (1999) (unpublished)
12. T. Antoni et al. - KASCADE Collaboration, *Astrop. Phys.* (2002), in press (astro-ph/0204266)